Supporting Information

Lithiated Interface of Pt/TiO_2 Enables an Efficient Wire-Shaped Zn-Air Solar Micro-Battery

Yao Luo,[a] *Panpan Li* [b,*] *and Zhaoyu Jin* [c,*]

[a.]State Key Laboratory of Biotherapy and Cancer Center, West China Hospital, Sichuan University, and Collaborative Innovation Center for Biotherapy, Chengdu 610041, P. R. China.

[b.]College of Materials Science and Engineering, Sichuan University, Chengdu 610065, P. R. China. Email: panpanli@scu.edu.cn

[c.]Institute of Fundamental and Frontier Sciences, University of Electronic Science and Technology of China, Chengdu 610054, P. R. China. Email: zjin@uestc.edu.cn

Experimental details

TiO_2 nanotube (TNT) array wire electrode. Ti wire (diameter: 0.2 mm, length: 3.0 cm) was first washed in diluted ethanol for 5 min under ultrasonic condition to remove the grease on the surface. Afterward, the TNTs were grown in-situ on the Ti wire by a well-established two-step anodic oxidation method.[1-3] Briefly, the pre-treated Ti wire was set as the anode and immersed into an ethylene glycol electrolyte containing 0.5 wt% NH_4F and 2 vol% deionized water with the length of 1.0 cm, while a graphite plate (4.0 cm^2) was also placed as the cathode. The first step of the anodic oxidation was conducted at 60 V by a direct-current power for 30 min, after which the grown TNTs were ultrasonically removed in deionized water. In the second step of the anodic oxidation, the Ti wire was treated at the same condition with the first step but only the voltage was 50 V. after 30 min, the TNTs were covered on the surface of the Ti wire and annealed at 450 ℃ for 1 h to increase their crystallinity.

Doping Li into TiO_2 nanotubes (Li-TNT). Lithium ions were inserted into the titania via an electrochemical approach in accordance with the previous reports.[4-6] In a typical process, three-electrode configuration was adopted with the TNT modified Ti wire as working electrode, Ag/AgCl electrode as reference electrode and Pt plate as counter electrode. An Autolab 101 potentiostat/galvanostat (Metrohm, Switzerland) supplied the constant-potential chronoamperometry in 2.0 M $LiNO_3$ solution at -1.2 V for 10 s, as well as the electrode was taken out, washed with water for several times and dried in the air. The color of the TNT film was changed from light blue to dark blue.

Electrodeposition of Pt nanoclusters. Li-TNT modified wire-shaped electrode was then cathodically treated in 1.0 mM H_2PtCl_6 aqueous solution for 20 s within the current-constant mode

(4 mA cm^{-2}). Consequently, the electrode was rinsed by water and dried at the room-temperature, of which the surface became dark grey after the successful deposition of Pt nanoclusters.

Characterizations. Scanning electron microscopy (SEM) analysis was carried out on a field emission Hitachi S4800 microscope (Japan). Spherical Aberration-Corrected Transmission electron microscopy (AC-TEM) images were recorded by a FEI Titan Themis 200 Microscope (USA). X-ray diffraction (XRD) analysis was performed on a Fangyuan DX-1000 powder X-ray diffractometer (China) with Cu Ka radiation at 40 kV. X-ray photoelectron spectra (XPS) were acquired with Kratos AXIS ULTRA DLD Photoelectron Spectroscope (UK) with element carbon as internal standard. Ultraviolet-Visible (UV-Vis) data were acquired using a Shimadzu UV3600 spectrometer (Japan).

Electrochemical measurements. All electrochemical tests for three-electrode system were carried out on a computer-controlled Autolab PGSTAT 128N potentiostat/galvanostat (Metrohm, Switzerland) in a 0.2 M phosphate buffer solution (pH = 7.0). In regard to the wire-shaped battery assembly, the negative electrode was fabricated by the electrodeposition of Zn in 0.5 M $ZnSO_4$ at -2.5 V for 10 min, after which the positive (diameter: 0.2 mm, length: 1.0 cm) and negative (diameter: 0.2 mm, length: 1.0 cm) electrode were parallelly immobilized on a flexible polyethylene terephthalate (PET) film with a gap of ca. 0.1 mm. The neutral gelled electrolyte, containing 1.0 g polyvinyl alcohol (PVA), 10 mL deionized water, 0.2 M acetate solution (pH = 7.0) and 0.05 M zinc acetate, was dipped onto electrodes and the gap and dried for ~ 2 hours in the air. The micro-battery performance testing was conducted under an AM 1.5G simulated solar light irradiation (100 mW cm^{-2}). Moreover, the flexible solar cell was commercially purchased from WARMSPACE company (China) and electrically contact with our assembled micro-battery.

Computations. The density functional theory (DFT) calculations were performed through the Cambridge serial total package (CASTEP).[7] The generalized-gradient approximation (GGA) in the Perdew−Burke−Ernzerhof for Solid (PBE-Sol) form with a cutoff for the plane waves of 340 eV was employed. We used 2 × 2 × 1 unit cells of anatase TiO_2 and Pt for geometric optimization, Li doping was conducted by replacing the Ti atom at the vertex site of the TiO_2 supercell. The k-points grid of 3 × 3 × 1 was used for calculating the densities of states and the thickness of vacuum space was set to be 15 Å.

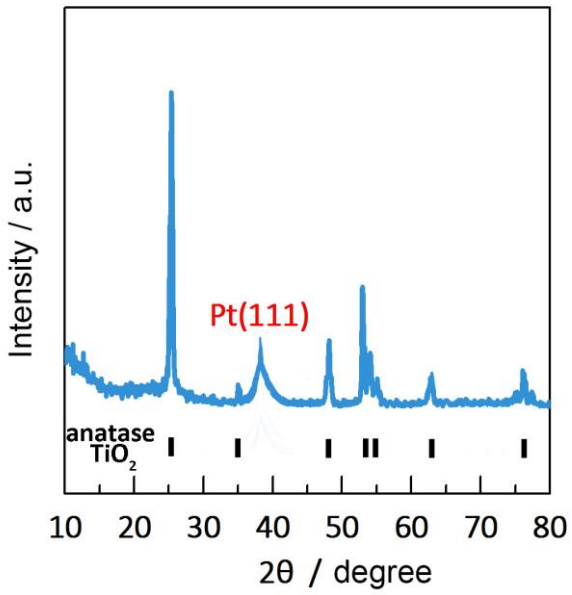

Figure S1. XRD pattern of the Li-TNT@Pt sample. The diffraction peak at ~38° is assigned to Pt(111), while other peaks are well matched with the anatase TiO_2.

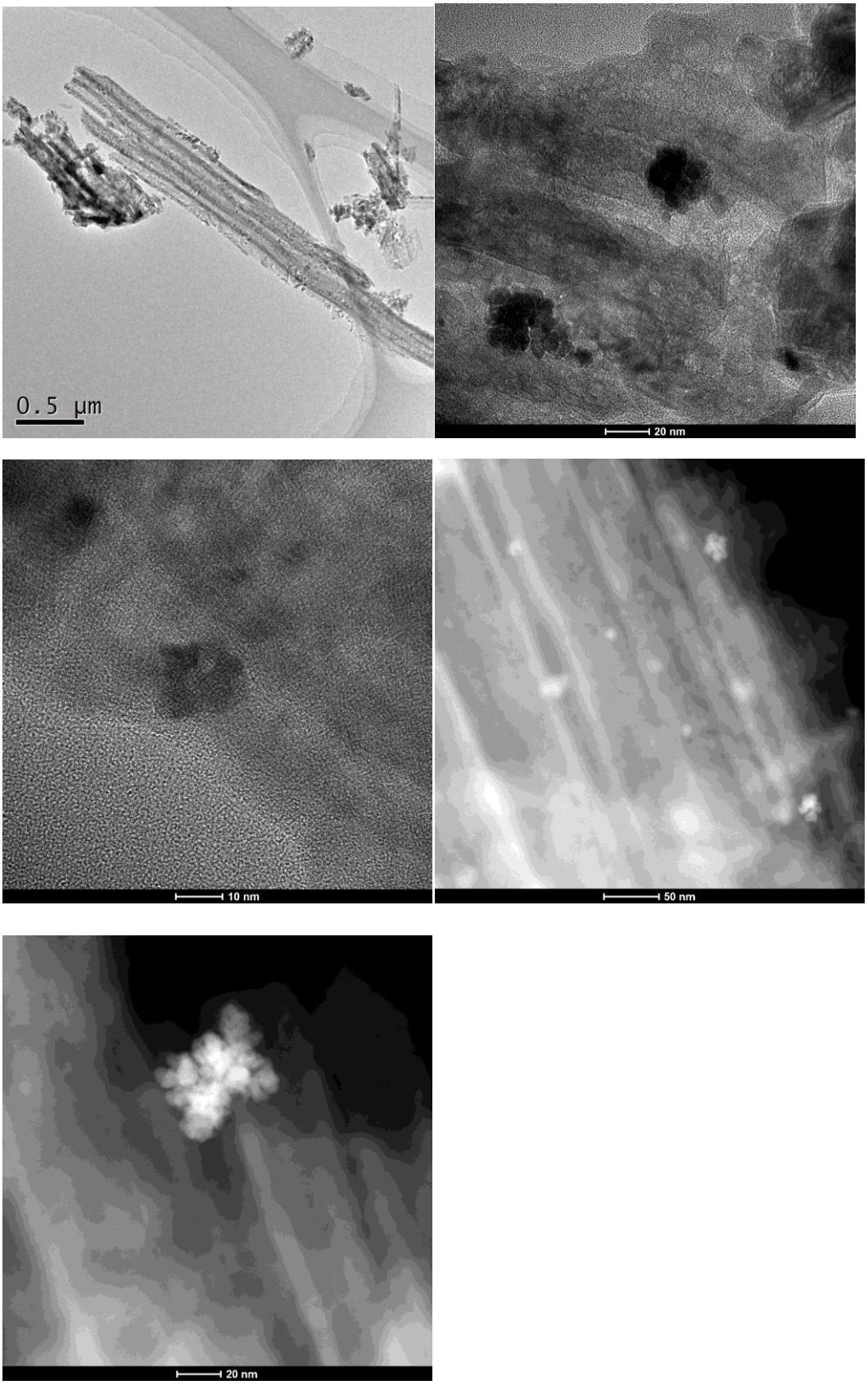

Figure S2. TEM and HAADF-STEM images of the Pt modified nanotubes. The sample was collected from the Li-TNT@Pt modified wire electrode.

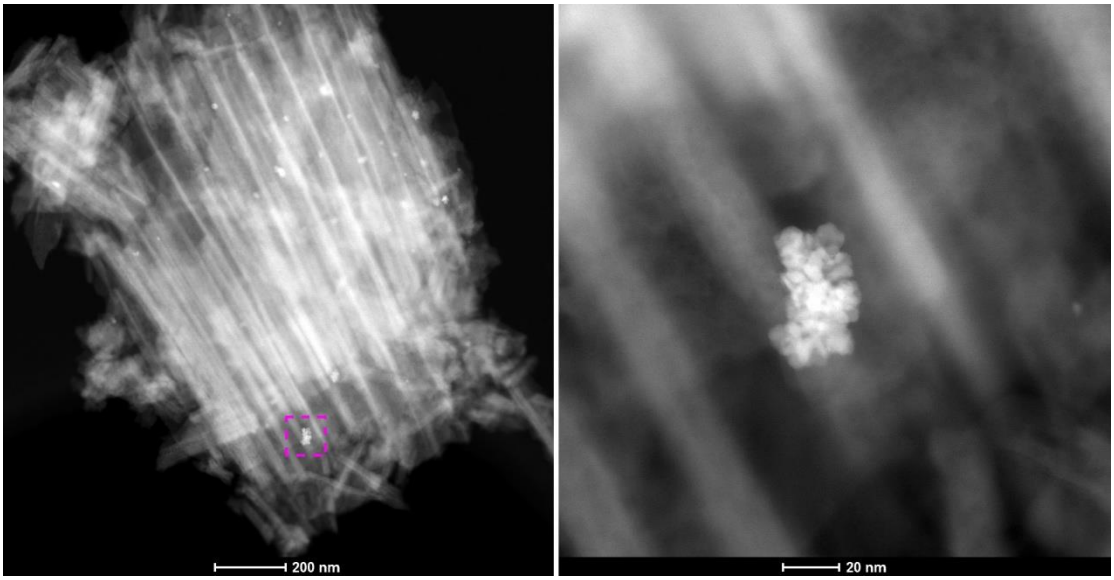

Figure S3. HAADF-STEM images of the Pt nanoclusters distributed on the surface of Li-TNT (left). Right figure illustrates an enlarged image of the area marked with the magenta dash box in the low-magnification image.

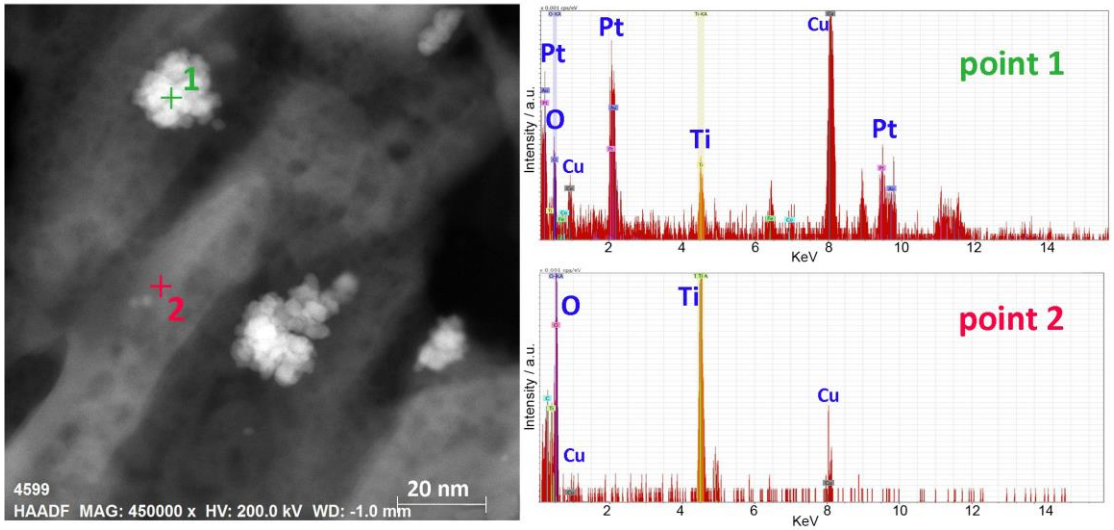

Figure S4. EDX point scanning for point 1 and point 2. The apparently different element content at point 1 and 2 reveals the bright area is the Pt nanocluster. It seems that there are some trace impurities, such as Fe and Co, existed in the Pt clusters. They are considered to come from the reagent of H_4PtCl_6, which is hard to avoid in the fabrication procedure. However, we used XRF to examine the precise content of these impurities, where the result shows Fe and Co contents are only 0.023 wt% and 0.011 wt%, respectively. In this regard, such low concentration of Fe and Co, we believe, will not bring obvious effect on the ORR and PEC performance in this study.

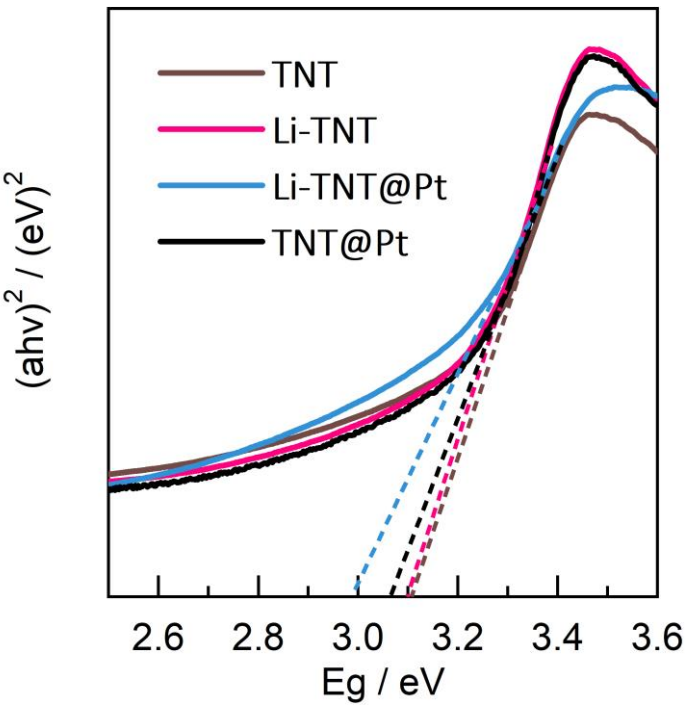

Figure S5. Optical bandgap fitting of TNT, Li-TNT, TNT@Pt and Li-TNT@Pt obtained from UV-Vis spectra.

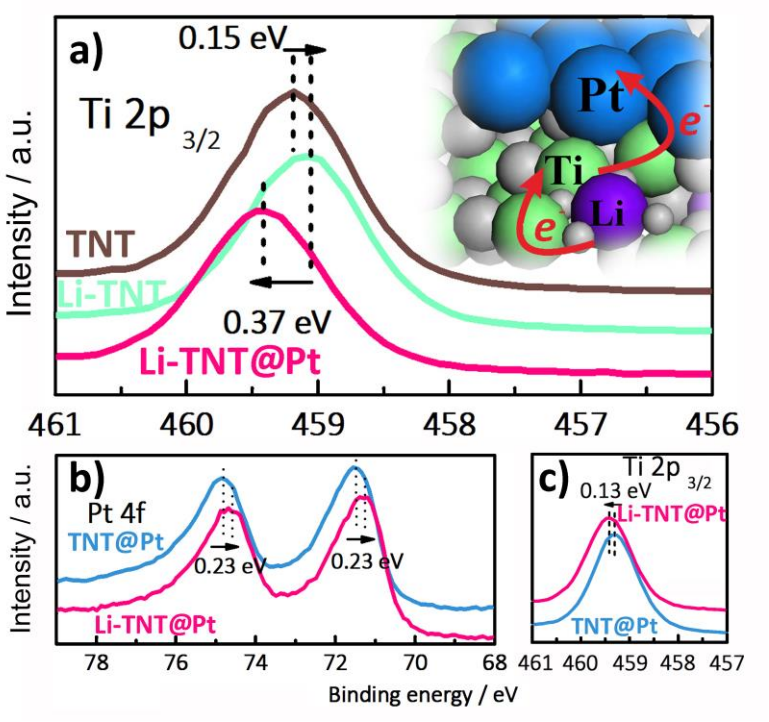

Figure S6. XPS spectra of a) Ti $2p_{3/2}$ and b) Pt 4f for TNT, Li-TNT and Li-TNT@Pt electrodes; c) Ti $2p_{3/2}$ for the Li-TNT@Pt and TNT@Pt.

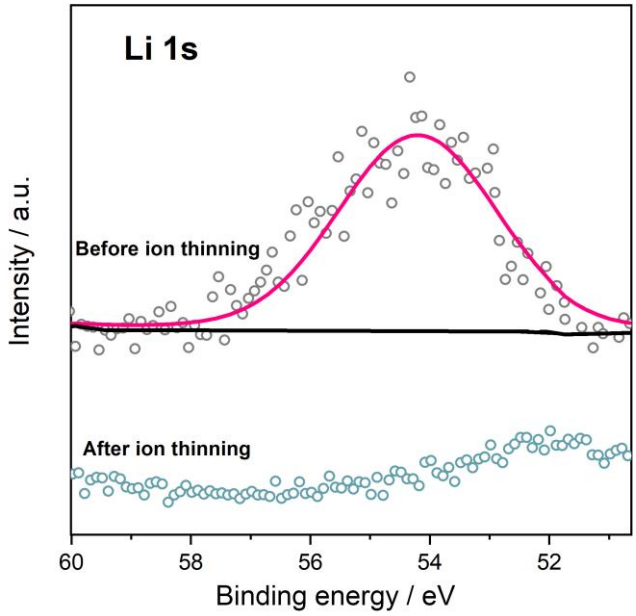

Figure S7. XPS spectra of Li 1s for the Li-TNT@Pt sample before and after Ar^+ thinning (5 s).

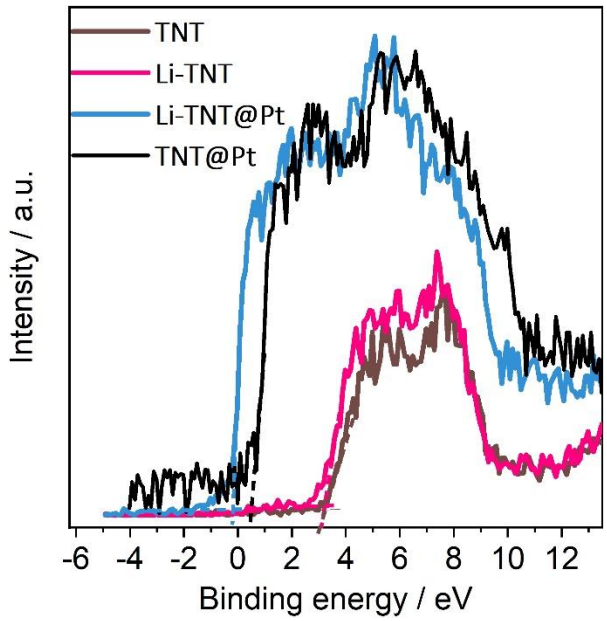

Figure S8. Valence-band XPS spectra of TNT, Li-TNT, TNT@Pt and Li-TNT@Pt. The results suggest the Li doping will not change the valence-band of the photoanode, while the surface energy level shows the significant increase on the of valence-band after the deposition of Pt, indicating the Fermi level of metallic platinum.

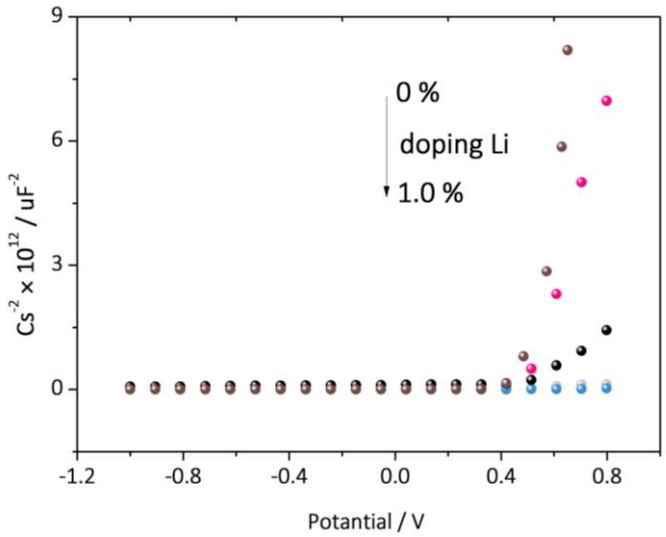

Figure S9. Mott-Schottky plots of the TiO_2 nanotubes electrode with different doping amount of Li (0, 0.1, 0.2, 0.4, 0.6, 0.8, 1.0 %).

The calculation method for the carrier concentration ($C_{carrier}$) is according to the equation[8]:

$$N_i = \left(\frac{2}{e\varepsilon\varepsilon_0}\right)\left(\frac{d\left(\frac{1}{C^2}\right)}{d(U_s)}\right)^{-1}$$

where e is the elementary charge value; ε_0 is the permittivity of the vacuum; ε is the relative permittivity of the semiconductor; U_s is the applied potential; C is the space charge capacitance in the semiconductor.

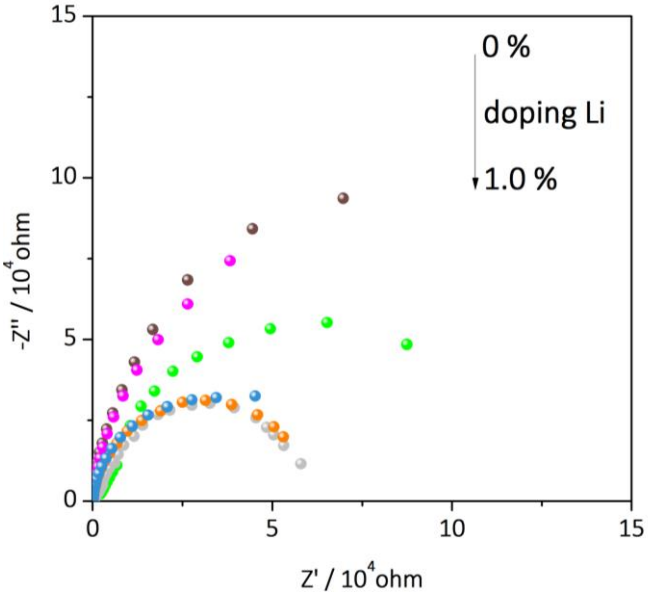

Figure S10. EIS plots of the TiO_2 nanotubes electrode with different doping amount of Li (0, 0.1, 0.2, 0.4, 0.6, 1.0 %) under solar irradiation. The calculation of R_{ct} is according to the equivalent circuit: $R_s(R_{ct}C)$. The applied potential is 0.3 V vs. Ag/AgCl.

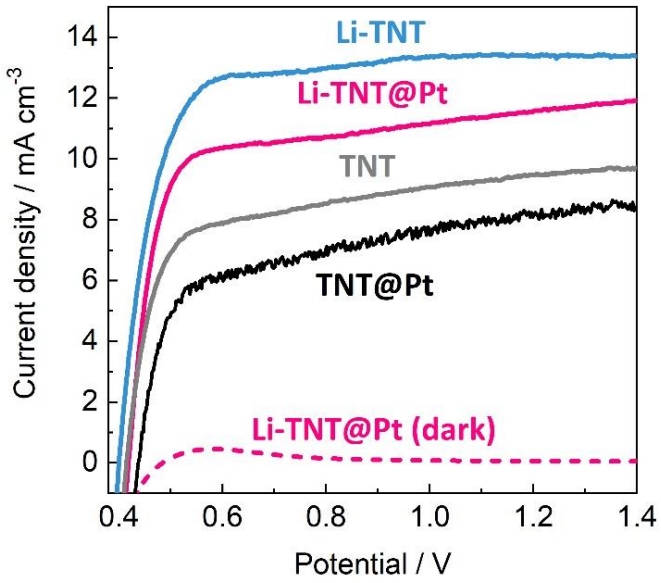

Figure S11. Photoelectrochemical water oxidation measurement for different electrodes.

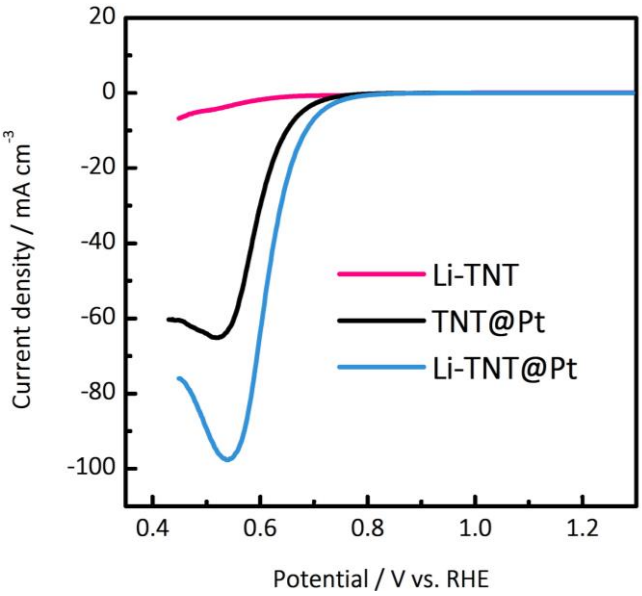

Figure S12. Polarization curves of oxygen reduction.

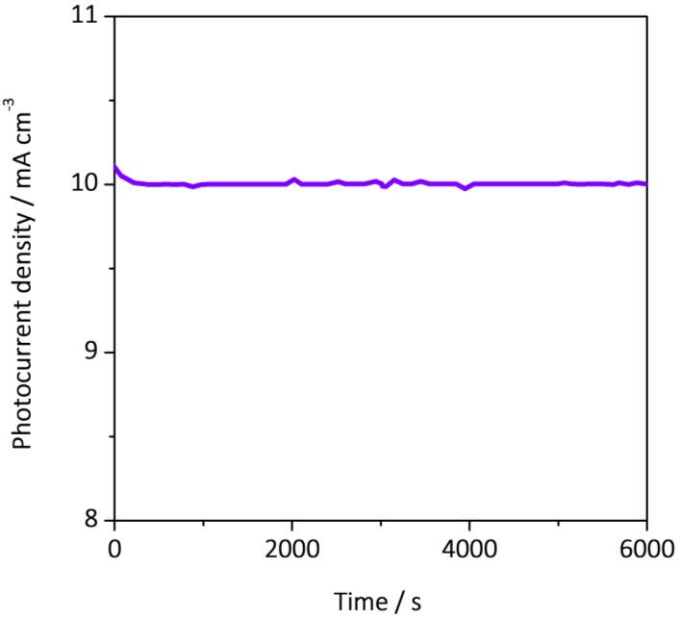

Figure S13. Photocurrent stability of Li-TNT@Pt under an AM1.5G solar light irradiation.

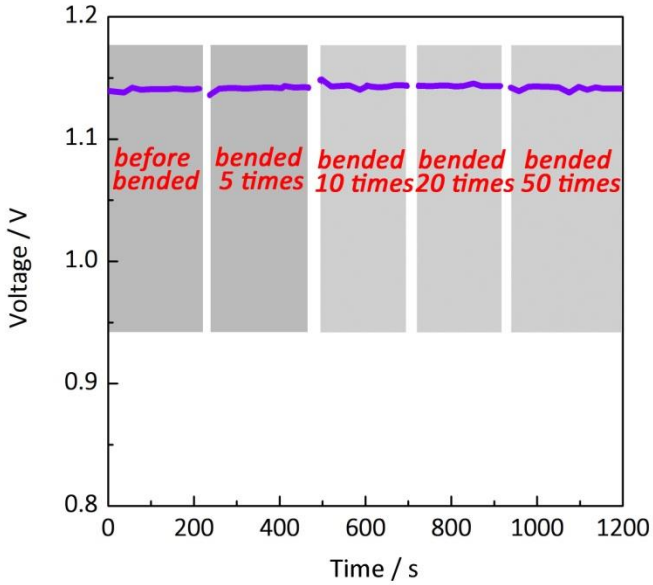

Figure S14. The discharge potential versus time curves for the battery before and after 5, 10, 20 and 50 times bended; the bending angle for per time is 90°.

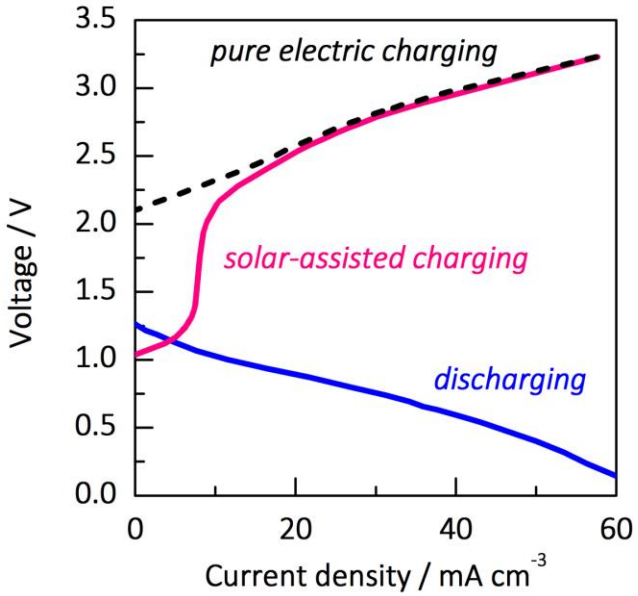

Figure S15. Polarization curves of the Zn//Li-TNT@Pt micro-battery.

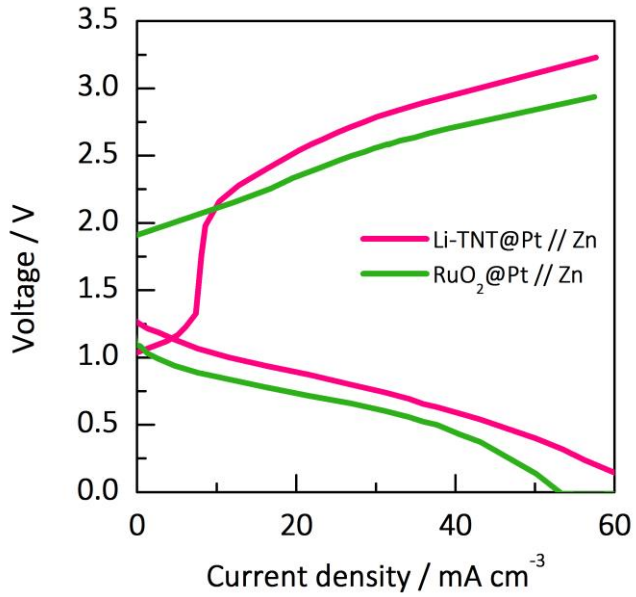

Figure S16. Charge and discharge I-V curves for conventional Zn-air battery and the proposed solar battery.

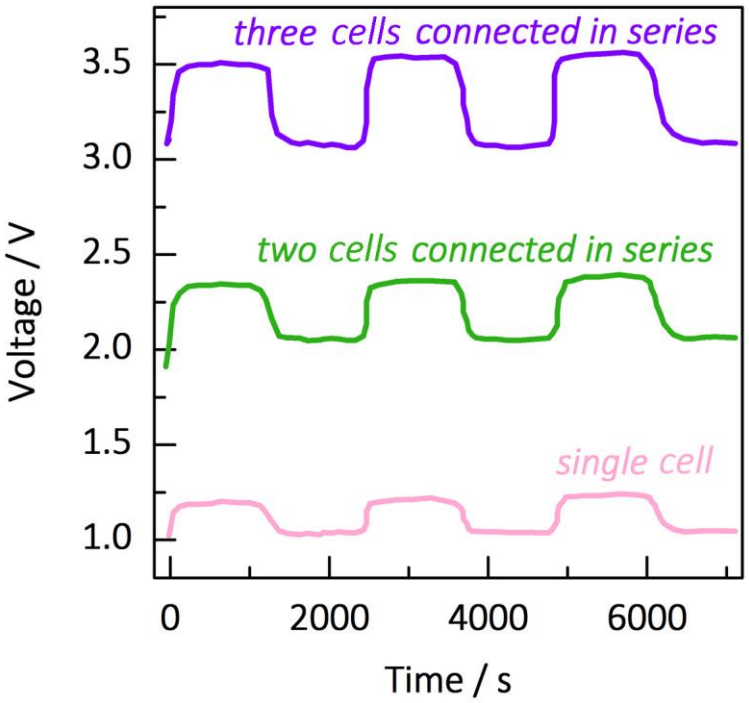

Figure S17. Charge-discharge voltage profiles of single, two and three cells in series connection.

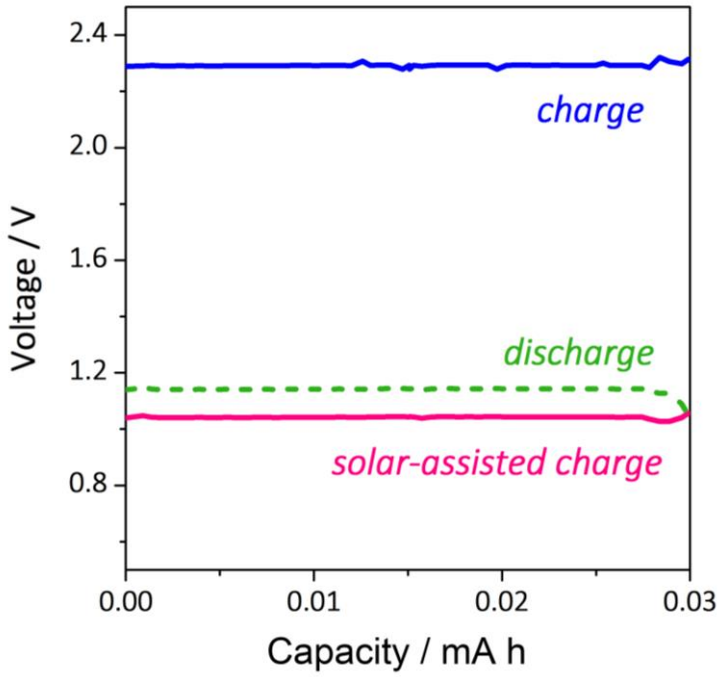

Figure S18. Charge profiles with and without solar irradiation and discharge profile at the current density of 1.6 mA cm^{-3}.

References:

1. Z. H. Zhang and P. Wang, *Energy Environ. Sci.*, 2012, **5**, 9948-9948.
2. H. Li, J. Chen, Z. Xia and J. Xing, *J. Mater. Chem. A*, 2015, **3**, 699-705.
3. P. Mazierski, M. Nischk, M. Gołkowska, W. Lisowski, M. Gazda, M. J. Winiarski, T. Klimczuk and A. Zaleska-Medynska, *Appl. Catal. B: Environ.*, 2016, **196**, 77-88.
4. B. H. Meekins and P. V. Kamat, *ACS Nano*, 2009, **3**, 3437-3446.
5. Y. Xin, Y. Cheng, Y. Zhou, Z. Li, H. Wu and Z. Zhang, *Chem. Commun.*, 2016, **52**, 4541-4544.
6. P. Li, Z. Jin and D. Xiao, *Energy Storage Mater.*, 2018, **12**, 232-240.
7. S. J. Clark, M. D. Segall, C. J. Pickard, P. J. Hasnip, M. J. Probert, K. Refson and M. C. Payne., *Z. Kristallogr.*, 2005, **220**, 567-570.
8. Z. Zhang, L. Zhang, M. N. Hedhili, H. Zhang and P. Wang, *Nano Lett.*, 2013, **13**, 14-20.